DE-EE0006816.0000
Oregon State University
Advanced Laboratory and Field Arrays (ALFA) for Marine Energy

1. INTRODUCTION

This document presents the results from discrete element method (DEM) simulations of interface shear compared to previously published data from similar physical experiments. Rough shafts emplaced in granular assemblies are subjected to monotonic and cyclic loading and the results evaluated. The granular-continuum interface behavior for different anchor surface roughnesses is presented and compared to the work by Paikowsky et al. (1995) and Uesugi and Kishida (1986). Comparisons between DEM and physical experiments for cyclic loading are performed by considering anchor efficiency, degradations, and load magnitude.

The model is described in detail in the project report for Checkpoint 4.1.1, which also contains model input parameters, results from parametric analyses, and a sample model script. These items are not repeated herein.

2. SIMULATION OF STRAIN SOFTENING

2.1. Overview

For heterogeneous materials, failure will occur due to distributed damages during which the material has strain softening. Strain softening is a phenomena wherein stress will decline with increasing strains. The major causes of strain softening are heterogeneity and brittleness. Sand is a heterogeneous material. The stress in a sand assembly is transmitted by contacts among sand particles. The mechanism of strain softening consists of void redistribution or a loss of interparticle contacts. Strain softening stably exists in a certain region in the material within a well-defined shearing zone. For continuum counterface–soil interaction, the stresses within this shearing zone (which exists over some distance orthogonally adjacent to the continuum counterface) define the strength of the system.

2.2. Comparison to Paikowsky et al. (1995)

Paikowsky et al. (1995) performed simple and direct shear tests to determine the interface friction angles between granular materials and solid inextensible surfaces. Glass beads and Ottawa sands were used in their experiments. The material properties were shown in Table 1.

Table 1. Material properties used by Paikowsky et al. (1995)

Material	Size range (mm)	G_s
Glass beads	2.0	2.48
Ottawa sand	0.36-1.66	2.65

The authors defined the solid surface normalized roughness based on Uesugi and Kishida (1986). In their tests, the normalized roughness of the smooth solid surface at the interface is $R_n = (7.8 \pm 4.4) \times 10^{-4}$

and the normalized roughness of an intermediate solid surface at the interface is $R_n = (5.4 \pm 1.0) \times 10^{-2}$. The interface friction angles are changing along with the displacement to the critical state.

In the current work, the simulated evolution of interface friction angle with displacement is similar to that observed by Paikowsky et al. (1995) for a normalized surface roughness of 0.04 (e.g., glass beads interacting with intermediate surface). The comparison between the physical experiments of Paikowsky et al. (1995) and the current DEM simulation is shown in Figure 1.

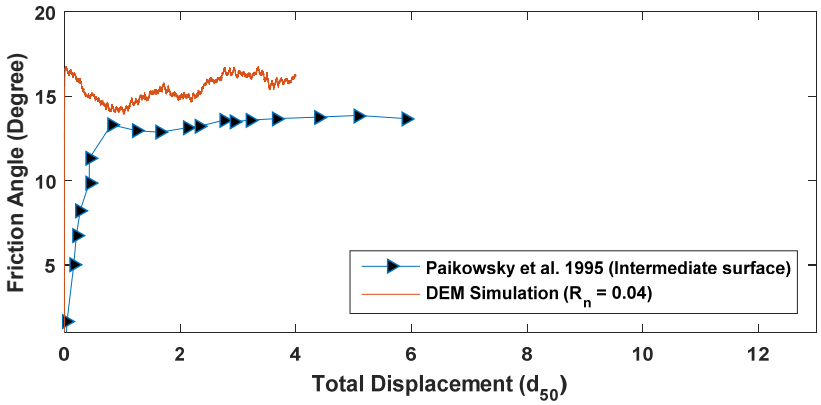

Figure 1. Comparison of interface friction angle from physical experiments on glass beads vs. DEM simulations, intermediate surface.

For the comparison in Figure 1, it is clear that the DEM simulation and physical experiment have similar trends. The tangential displacements are normalized by the particle mean size (d_{50}). The normalized surface roughness of the DEM simulation (0.04) and the physical experiment (0.054 ± 0.01) are nearly the same. The critical state interface friction angle for the DEM simulation is approximately $15°$ while that measured by Paikowsky et al. (1995) is $14°$. The most marked difference between the simulation and the test is the initial stiffness of the system is much higher for the DEM simulation than for the physical experiment, which requires a displacement of $0.8d_{50}$ to reach critical state. This is also apparent for the case of a rough counterface surface ($R_n = 0.4$), which is shown in Figure 2.

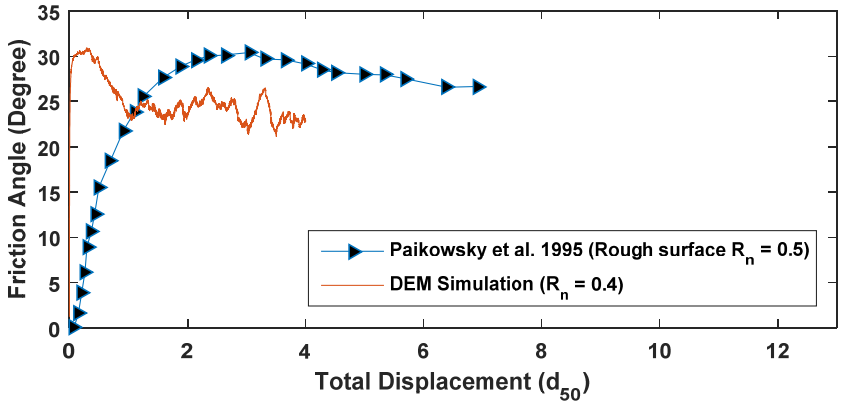

Figure 2. Comparison of interface friction angle from physical experiments on glass beads vs. DEM simulations, rough surface.

The critical state friction angle between glass beads and rough aluminum surface tested by Paikowsky et al. 1995 is $27°$, the value for DEM simulation under similar surface roughness is $24°$. The maximum interface friction angle for both experimental test and DEM simulation is $30°$.

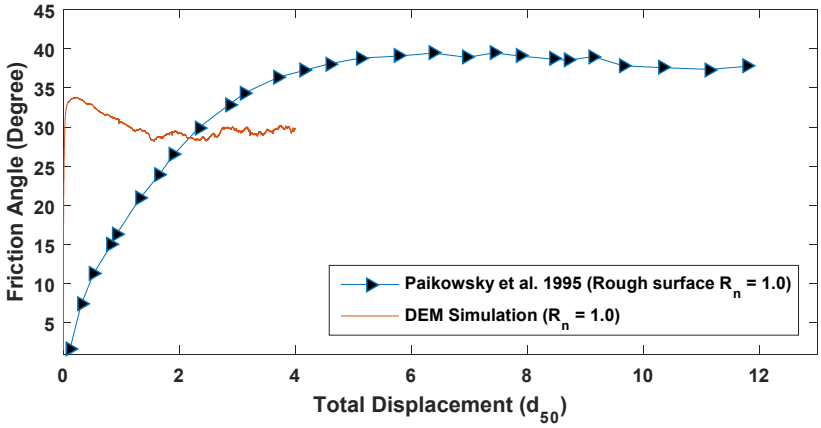

Figure 3. Comparison of interface friction angle from physical experiments on Ottawa sand vs. DEM simulations, rough surface.

If we compare the DEM simulation with the test performed by Paikowsky et al. (1995) for the interface between Ottawa sand and rough aluminum, the difference is slightly larger, as shown in Figure 3. The maximum interface friction angle for DEM simulation with surface normalized roughness $R_n = 1$ is $33.5°$, while that for the physical test on Ottawa sand at the same counterface roughness is $39°$. The critical state interface friction angles are $29°$ and $36°$ for numerical and physical experiments, respectively. This is not difficult to understand. The particle shapes in the DEM simulations are not the same as those Ottawa sand. This is an area that still requires further investigation. Nonetheless, the model clearly captures the strain softening response observed in physical experiments and overall, the trends are similar.

Paikowsky et al. (1995) also investigated the effects of normalized surface roughness, R_n, on the peak angle of interface friction for various glass bead-continuum systems (i.e., differing particle sizes and surface geometries). These results, along with comparable numerical simulations, are presented in Figure 4. The trends shown in Figure 4 are in accordance with each other with the similar bilinear property. The peak interface friction angle is increasing with the increasing of normal roughness when normal roughness is smaller than 0.5. After that, the peak interface friction angle will not increase when increasing the normal roughness. More detailed model calibration would result in even better agreement with measured results, but that is not the goal of the current work (i.e., to match a set of measured data exactly).

2.3. Comparison to Uesugi and Kishida (1986) and Implications for Internal Consistency

Uesugi and Kishida (1986) performed physical interface shear tests on the interface between different sands and mild steel using a simple interface shear apparatus. They considered the effects of counterface surface roughness, particle shape, and the median grain diameter (d_{50}) of the sand and proposed a normalized roughness that accounts for the scale of the surface features on the continuum counterface relative to the particle size. Three sands were tested. To quantify the effects of particle angularity on interface shear strength, they proposed a modified roundness parameter for the sand particles allowing

them to evaluate the maximum interface friction angles along with different surface roughness (see Checkpoint 4.1.1 report). Properties of the three sands are shown in Table 2.

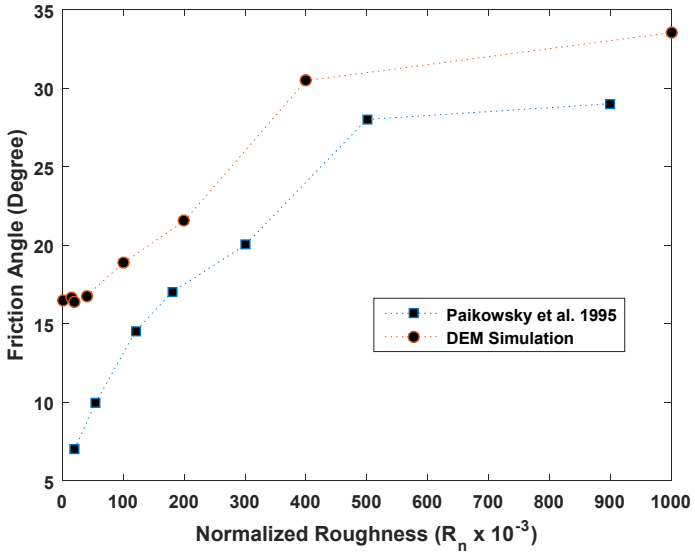

Figure 4. Peak interface friction angle as a function of counterface roughness

Table 2. Properties of the tested sands (after Uesugi and Kishida, 1986)

Sand Type	Particle Diameters (mm)	d_{50} (mm)	G_s	e_{min}	e_{max}	R_{mod}
Toyoura	0.11-0.25	0.18	2.65	0.604	0.991	0.27
Fujigawa	1.68-2.00	1.82	2.72	0.772	1.067	0.19
	0.50-0.59	0.54	2.72	0.763	1.148	
	0.07-2.00	0.54	2.72	0.532	0.94	
	0.15-0.18	0.16	2.74	0.768	1.117	
Seto	1.68-2.00	1.82	2.64	0.748	1.04	0.17
	0.50-0.59	0.54	2.64	0.737	1.15	
	0.07-2.00	0.54	2.64	0.535	0.737	
	0.15-0.18	0.16	2.64	0.78	1.245	

Plots of the maximum interface friction coefficient for the three sand types tested by Uesugi and Kishida (1986) exhibited a bilinear relationship of interface friction angle as a function of normalized roughness R_n (Figure 5). They showed that the interface shear resistance is proportional to the normal roughness until some critical value equal to the internal friction angle of the soil (i.e., this is the point where the failure moves away from the interface and into the bulk soil, because the weakest component of the system will always fail first).

Result from our DEM simulations are also presented in Figure 5 and bilinear response is observed. We note that this is somewhat remarkable and is indicative that the model is correctly capturing the problem physics. That is, the model has not been tuned or calibrated in any way to elicit this type of response –

rather, the same phenomenon that results in the bilinear response observed in the physical tests also results in bilinear response in the numerical tests. We note that this type of behavior would not be observed in any satisfyingly robust way in either an FEM or limit equilibrium model.

On initial observation, Figure 5 appears to imply that the DEM model is not reasonable reproducing the results for the three sands tested by Uesugi and Kishida (1986). However, it is important to note that the levels of the plateaus of the bilinear trends are a function of material properties – that is, each is the peak angle of internal friction for that granular material. According to the Uesugi and Kishida (1986) definition of modified roundness, the spheres used in the DEM simulation have a roundness of one. Because peak internal friction angle for a granular material generally decreases with increasing roundness, we expect that the DEM assembly will have the lowest strength of the four materials. Thus, if the shear strength for each of the four granular materials was known, a more appropriate plot would be the interface friction angle *normalized by* the peak internal friction angle of the granular material, i.e., δ'/ϕ'. This is the subject of ongoing work.

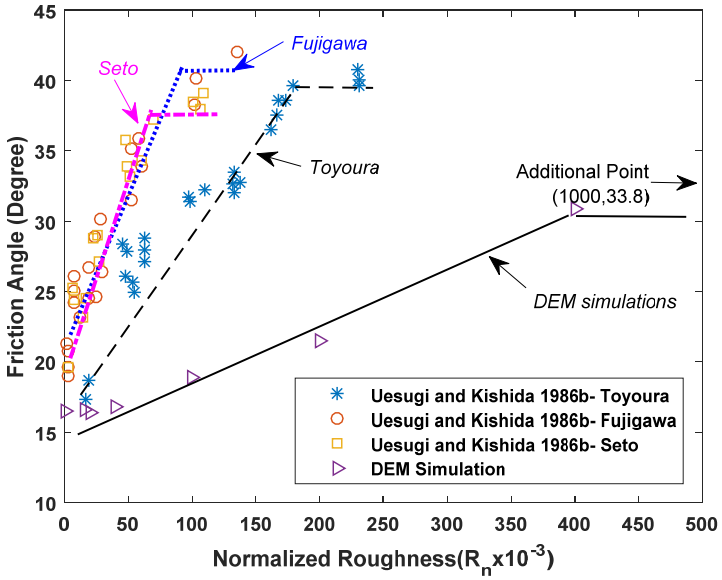

Figure 5. Interface friction angle as a function of normal roughness; comparison between the physical tests of Uesugi and Kishida (1986) and our DEM simulations

The DEM simulations exhibited both strain hardening and strain softening response (Figure 6). The interface friction angles reach their peak value at small deformations during shear for all the interface roughness values considered, and then experience softening to critical state. Interphase system strength generally increases with increasing counterface roughness, as expected. In summary, Figure 6 indicates internally consistent model results across a range of counterface roughness values.

2.4. Comparison to Uesugi at al. (1990) and the Interplay Between Roughness and Friction

Uesugi et al. (1990) performed physical experiments on soil-concrete interfaces and evaluated the residual interface friction coefficients under different interface concrete surface roughness. They used a simple shear type apparatus and applied monotonic loading with constant velocity tangent to the counterface. Toyoura sand (see Table 2) was used for testing. The residual and peak interface friction

angles for different surface roughnesses that they measured are presented in Table 3. Comparable results for the current DEM simulations are presented in Table 4.

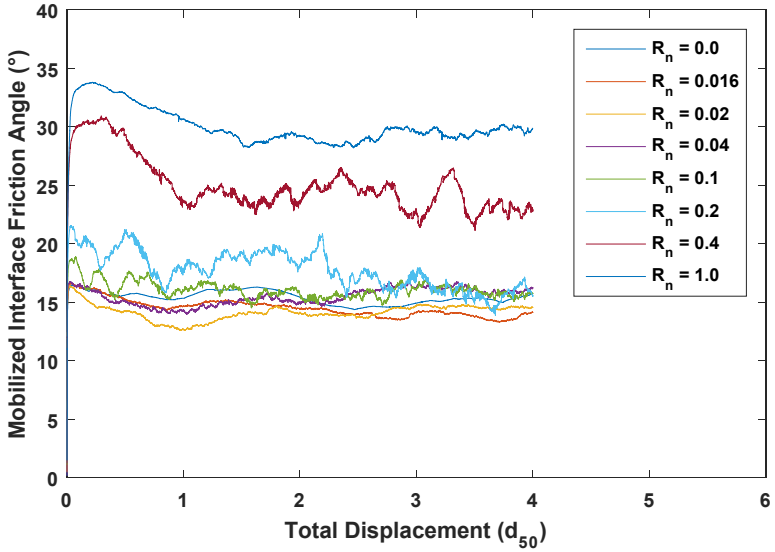

Figure 6. The effects of normaized counterface roughnesss on the mobilized friction interface friction angle-displacement behavior

Table 3. Residual (δ_r) and peak (δ_p) interface friction angles for varying roughness (Uesugi et al. 1990)

R_n ($\times 10^{-3}$)	δ_r (°)	δ_p (°)	δ_r/δ_p
83	29.7	33.4	0.89
106	31.0	37.6	0.82
167	30.5	39.0	0.78

Table 4. Residual (δ_r) and peak (δ_p) interface friction angles for varying roughness (DEM simulations)

R_n ($\times 10^{-3}$)	δ_r (°)	δ_p (°)	δ_r/δ_p
0	14.1	16.5	0.86
16	14.0	16.7	0.84
20	14.2	16.4	0.86
40	15.9	16.8	0.95
100	16.0	18.9	0.85
200	17.7	21.5	0.82
400	22.7	30.5	0.75
1000	29.0	33.5	0.87

The ratios of residual and peak interface friction angles for similar normalized roughnesses are consistent for the physical and numerical tests. Negussey, et al. (1989) showed that the difference in magnitude between peak and residual interface friction angles increases with the angularity of the counterface. This phenomenon is apparent in the DEM simulations and can be better understood by considering the differences in interface material parameters selected in the simulation, as discussed below.

A series of parametric simulations were used to assess the effects of changing the values of shaft friction, which occurs at a smaller spatial scale than roughness. The maximum interface friction angle does not increase significantly if the shaft friction coefficient is increased (Figure 7) compared to the changes observed as a function of counterface surface roughness shown in Figures 5 and 6.

However, it is expected that the residual interface friction angle and initial stiffness are a function of shaft friction. High shaft friction values result in rapid mobilization of shear forces from the static state because there is little slip between particle contacts and the otherwise "smooth" (i.e., frictional, but not rough) counterface material. Similarly, at large displacements, it is expected that higher counterface friction values will serve to increase the residual interface friction angle of the system due to stick-slip behavior at particle contacts along the shaft. These phenomena are currently under investigation. We expect that effectively capturing the interplay between friction and roughness and their combined effects on system response will be critical for the successful modeling of the soil-anchor-mooring line system.

Referring to the work of Potyondy (1961), the skin friction between various soils and construction materials is considered. He used a strain-controlled shear box and a stress-controlled shear box to set up several hundred physical experiments to analyze the magnitudes of shin friction and the relationship between skin friction and the strength of a soil. Potyondy (1961) measured the interface strength of sand against a variety of materials – wood, concrete, and steel – and also assessed variations within material type (Table 5). In this manner, the combined effects of friction, roughness, and hardness are assessed, but it is possible to tease out a qualitative understanding of the influence of each individually. Specifically, the Potyondy (1961) data imply that material friction is perhaps more important than roughness (looking at values for smooth surfaces across material type), but that hardness clearly plays a role in system response for changing roughness at constant friction (the difference between smooth and rough steel versus the other materials).

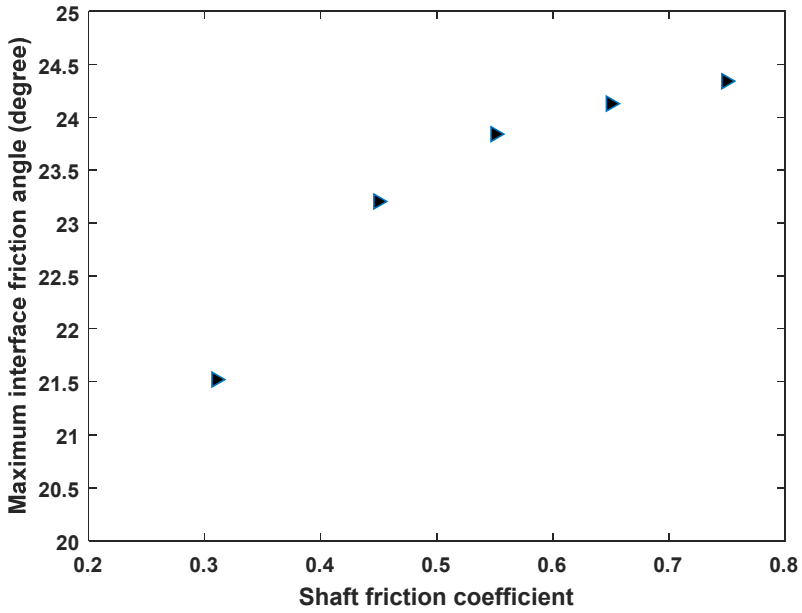

Figure 7. Maximum interface friction angle for varying shaft friction coefficients (DEM simulations)

Table 5. Interface friction angle between sand and different materials (after Potyondy 1961)

Normal Load	1000 psf			3000 psf		
Material	ϕ	δ	δ / ϕ	ϕ	δ	δ / ϕ
Smooth steel	44.5°	24.2°	0.543	44.5°	24°	0.55
Rough steel	44.5°	34°	0.77	44.5°	33.7°	0.78
Wood parallel to grain	44.5°	35°	0.79	44.5°	33.3°	0.77
Wood at right angles to grain	44.5°	39°	0.88	44.5°	38.5°	0.89
Smooth concrete	44.5°	39.5°	0.89	44.5°	38.5°	0.89
Rough concrete	44.5°	44°	0.99	44.5°	42.5°	0.98

It is clear that the rougher and more frictional the construction material, the higher the interface friction angle. The rough concrete gave a highest interface friction angle which is almost identical to the fiction angle of sands. The DEM simulation results presented in Figures 5 and 7 show that the maximum interface friction angle is approaching some maximum value (i.e., the internal friction angle of the bulk granular material) with both increasing shaft roughness and friction.

3. GRANULAR STRUCTURE EVOLUTION DUE TO CYCLIC LOADING

Wave energy converters (WECs) are floating facilities with mooring lines tied to seabed anchors. On the water surface, ocean waves are clearly repeated, having a range of regular amplitudes and periods. In addition to these repeated, regular waves, additional excitations may occur, corresponding to infrequent environmental stimuli (e.g. earthquakes, storms, variable currents) and consisting of cyclic loads applied to the WECs in addition to the regular loading. All of these excitations are passed to the anchors via the compliant mooring system.

The most severe cyclic loads consist of many irregular amplitudes and uncertain periods which are difficult to reproduce in field and laboratory or soil element tests. More commonly, uniform repeated loading with square waveforms having specified periods and regular amplitudes are used because of their complex (indeed, infinite) frequency content. In the current work, considering the fact that mooring lines cannot apply compressive forces to an embedded anchor, one-way repeated square loads are simulated.

According to O'Loughlin et al. (2004), Medeiros (2011), and Lieng et al. (2000), anchor efficiency ranges from 3-9, meaning that the holding capacity of the anchor is 3-9 times of the anchor dry weight. In order to model the process when there is no tension force on the mooring lines, a velocity of $0.11v_p$ to $0.33v_p$ (where v_p is pullout velocity) should be applied downward. In the current simulations, a value of $0.20v_p$ is used. Thus, applied waves having a frequency of 1 Hz with pullout velocities varying from +0.1 m/s (pullout) to -0.02 m/s (relaxation) are employed herein. A sample waveform is shown in Figure 8.

Preliminary simulations based on the applied loads shown in Figure 8 are currently focused in three major areas:

- Comparison of system behaviors under constant loading (quasi-static) and cyclic loading (dynamic) conditions.

- Evaluation the degradation of interface strength for different soil-continuum interface friction angles. Soil-continuum interface friction angles increase with increasing continuum surface roughness; thus, the higher the surface roughness, the higher the relative degradation of interface strength.
- Different cyclic load magnitudes, which can be simulated by applying velocities with different magnitudes.

The following results and discussions are based on the above three items.

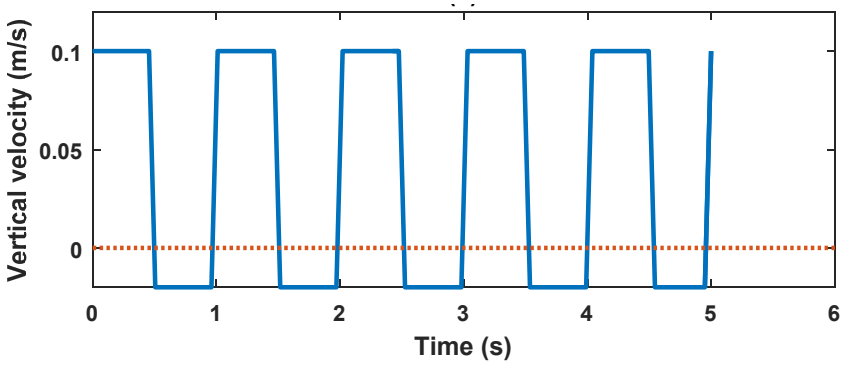

Figure 8. One-way repeated loading type

Cyclic bearing capacities should support structures while keeping deformation within acceptable limits. According to the work of Matlock and Homquist (1975) on cyclic loading tests on piles, the pile loading capacity and stiffness during cyclic loading will severely degrade due to soil remolding along the pile shaft. Anderson et al. (2013) came to a similar conclusion. The current DEM model reproduces similar behavior (without calibration), as shown in Figure 9 below.

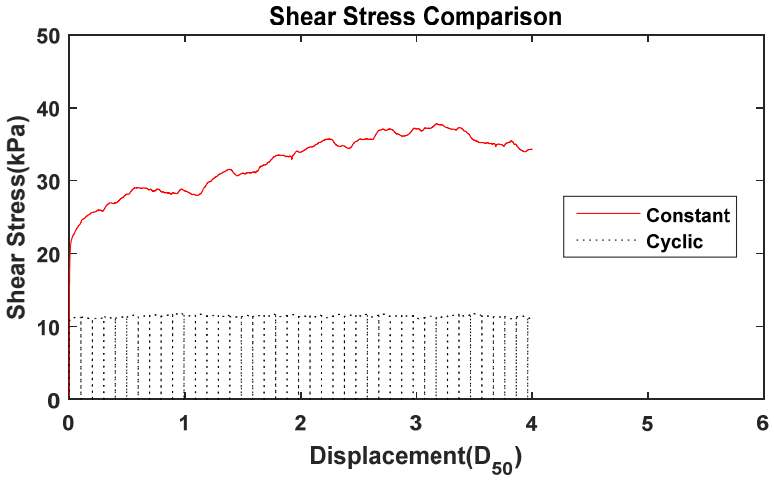

Figure 9. Comparison between constant loading and cyclic loading

Figure 9 shows that the shear stress during pullout is much smaller for cyclic loading than for constant loading. There is large cyclic degradation, consistent with the work of Grosch and Reese (1980), in which they measured the loading capacity of a pile compared to the undrained shear strength of the surrounding soil. The static loading capacity is 2.47-2.97 times that during cyclic loading. For the DEM simulations shown in Figure 9, the maximum holding capacity degradation factor is 3.18.

Varying load amplitudes are simulated by applying different velocities to the shaft walls. In the prelimimary sensitivity analyses, three different pullout velocities are applied to the anchor shaft walls: 0.16, 0.2, and 0.24 with units of d_{50}/s. Shear stress versus shaft displacement for these three conditions is shown in Figure 11. The shear stresses for the three different cyclic loadings are comparable, implying that shear stress is not overly sensitive to the loading velocity.

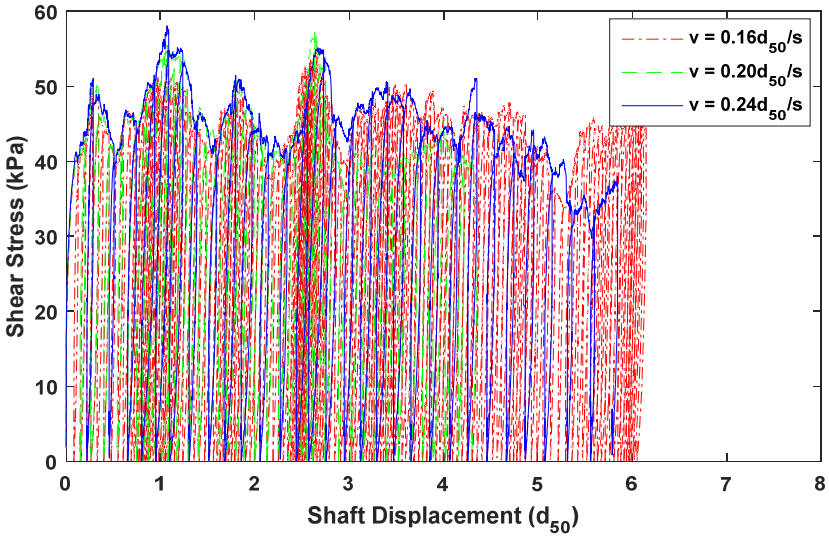

Figure 10. Anchor shaft shear stress under different cyclic loadings

To assess the underlying physics that drives strength degradation during cyclic loading, assembly porosity is monitored with the increase of the number of loading cycles. The model is divided into four concentric subzones, as shown in Figure 11. Porosity trends within each subzone during cyclic loading are presented in Figure 12.

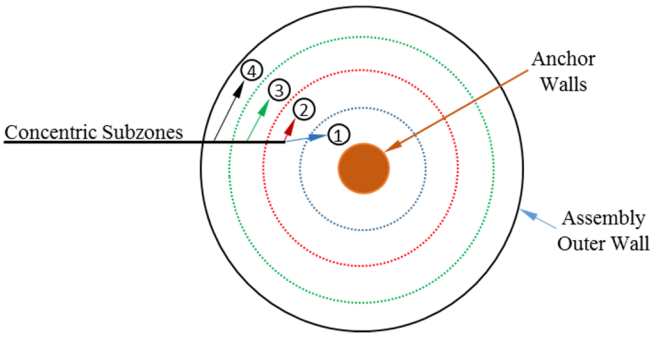

Figure. 11. Subzones of zone between shaft and cylinder wall

The porosity of subzone 1 is slightly larger than the other subzones and increases slightly more with cyclic loading. generally, cyclic loading appears to not significantly influence porosities in regions removed from the shaft. However, it has been shown (Agnolin and Roux 2007) that coordination number (the average number of contacts per particle) is a much better indicator of macroscale behavior than porosity. Unfortunately, it is not generally feasible to measure coordination number in real physical systems, porosity is implicitly used as a surrogate (albeit, an admittedly poor one sometimes). Figure 13 shows the coordination number in each subzone decreasing with the cyclic loading. The subzone adjacent to the

anchor shaft loses more contacts per particle than other subzones, implying a loss of shear strength, since stresses are transmitted via forces at particle contacts. Thus, we conclude that during cyclic loading, yielding will result more in the loss of contacts than in changing porosity. This is compelling behavior that we are continuing to study.

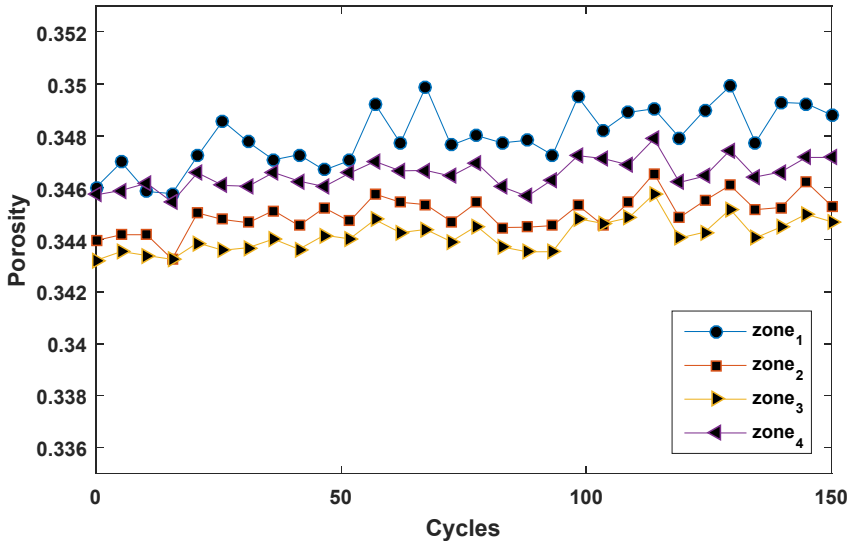

Figure 12. Subzone porosities along with cyclic cycles

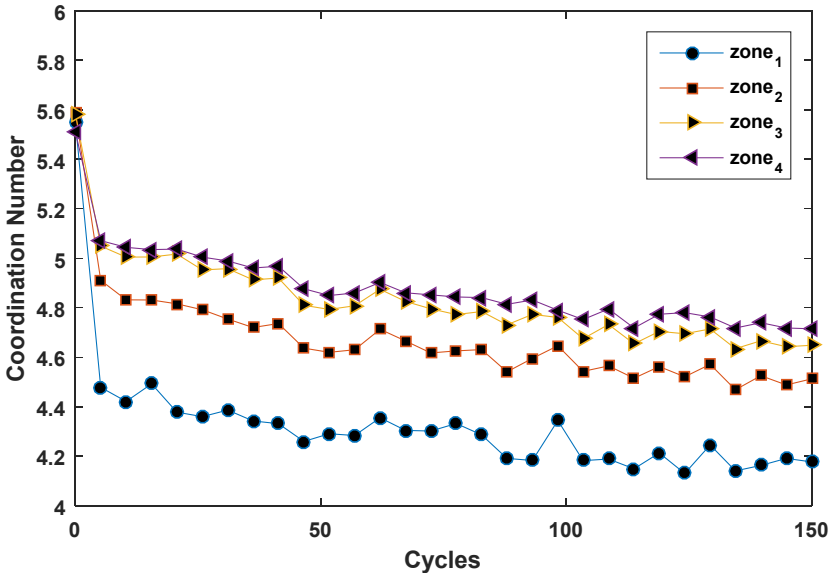

Figure 13. Coordination numbers of each subzone along with cyclic loading

4. SUMMARY AND PRELIMINARY CONCLUSIONS

This report focused on the comparisons between DEM simulations and physical experiments under constant loading conditions. Model response under cyclic loading was preliminarily investigated as well. The DEM model simulates measured three-dimensional interface shear behavior reasonably well. (We note here that, to our knowledge, simulations of this type have not been previously reported in the literature.) Comparable results between DEM simulations and physical tests performed by Paikowsky et

al. (1995) for different counterface roughnesses showed the allowable accuracies when considering the interface friction angles. Interface friction angles at failure under three different conditions were consistent:

1. glass beads vs. DEM, intermediate surface ($\delta = 14°$ vs $\delta = 15°$);
2. glass beads vs. DEM, rough surface ($\delta = 30°$ vs $\delta = 30°$); and
3. Ottawa sands vs. DEM, rough surface ($\delta = 39°$ vs $\delta = 36°$).

The interface friction angles along with different counterface roughnesses between DEM simulations and the results from physical experiments by Uesugi and Kishida (1986, 1990) were compared as well. Results showed that the interface friction angle along with normalized roughness has a bilinear behavior. The DEM simulations also exhibited this bilinear behavior (without calibration). At the current stage, the DEM model is robust not only qualitatively, but quantitatively.

Finally, DEM simulations under cyclic loading were performed to check shear strength degradation between constant loading and cyclic loading. Results showed that constant loading had a higher pullout resistance than that of cyclic loading. Further studies on cyclic loading are currently underway.

5. REFERENCES

Agnolin I, Roux I. (2007). “Internal states of model isotropic granular packings. III. Elastic properties.” *Physical Review E* 76:061304.

Andersen, K., A. Puech, and R. Jardine. "Cyclic resistant geotechnical design and parameter selection for offshore engineering and other applications." *Design for cyclic loading: Piles and other foundations, Proceeding of TC 209 Workshop–18th ICSMGE*, Paris. 2013.

Grosch, J.J. and L.C. Reese (1980). Field tests of small-scale pile segments in a soft clay deposit under repeated axial loading. In *Proc. 12th Offshore Technology Conference*, OTC 3869, pp. 143–151. Houston, TX.

Matlock, H., and Holmquist, D. V. (1976). A model study of axially loaded piles in soft clay. *Rep., American Petroleum Institute*, University of Texas at Austin.

Negussey, D., Wijewickreme, W. K. D., and Vaid, Y. P. (1989). Geomembrane interface friction. *Canadian Geotechnical Journal*, 26(1), 165-169.

Paikowsky, S. G., Player, C. M., and Connors, P. J. (1995). A dual interface apparatus for testing unrestricted friction of soil along solid surfaces. *ASTM Geotechnical Testing Journal*, 18(2), 168-193.

Potyondy, J. G. (1961). Skin friction between various soils and construction materials. *Géotechnique*, 11(4), 339-353.

Uesugi, M. and Kishida, H. (1986). Influential factors of friction between steel and dry sands. *Soils and Foundations*, 26(2), 33–46.

Uesugi, M. and Kishida, H. (1990). Friction between dry sand and concrete under monotonic and repeated loading. *Soils and Foundations*, 30(1), 115-128.